

A universal velocity dispersion profile for pressure supported systems: evidence for MONDian gravity across 12 orders of magnitude in mass

X. Hernandez¹, R. Durazo¹, B. Cervantes-Sodi², H. J. Ibarra-Medel¹ and O. Lopez-Cruz³

¹*Instituto de Astronomía, Universidad Nacional Autónoma de México, Apartado Postal 70–264 C.P. 04510 México D.F. México.*

²*Centro de Radioastronomía y Astrofísica, Universidad Nacional Autónoma de México, Campus Morelia, 58090 Morelia, Michoacán, México.*

³*Instituto Nacional de Astrofísica, Óptica y Electrónica (INAOE), Astrofísica, Luis Enrique Erro No.1, Tonantzintla, Pue., C.P. 72840, México.*

Released 14/06/2015

ABSTRACT

For any MONDian extended theory of gravity where the rotation curves of spiral galaxies are explained through a change in physics rather than the hypothesis of dark matter, a generic dynamical behaviour is expected for pressure supported systems: an outer flattening of the velocity dispersion profile occurring at a characteristic radius, where both the amplitude of this flat velocity dispersion and the radius at which it appears are predicted to show distinct scalings with the total mass of the system. By carefully analysing dynamics of globular clusters, elliptical galaxies and galaxy clusters, we are able to significantly extend the astronomical scales over which MONDian gravity has been tested, from those of spiral galaxies, to the much larger range covered by pressure supported systems. We show that a universal projected velocity dispersion profile accurately describes various classes of pressure supported systems, and further, that the expectations of extended gravity are met, across twelve orders of magnitude in mass. This observed scalings are not expected under dark matter cosmology, and would require particular explanations tuned at the scales of each distinct astrophysical system.

Key words: gravitation — stars:kinematics and dynamics — galaxies:star clusters:general — galaxies:fundamental parameters — galaxies:kinematics and dynamics — galaxies:clusters:general

1 INTRODUCTION

Within the context of modified gravity theories constructed to yield galactic dynamics in the absence of dark matter, one of the most convincing supporting arguments comes from the success of MOND in reproducing rotation curves of spiral galaxies e.g. Milgrom (1983), Swaters et al. (2010), McGaugh (2012). Both the flatness of the observed spiral rotation curves and the scaling of the asymptotic rotation with the fourth root of the total baryonic content, the Tully-Fisher relation, can be accurately reproduced across spiral galaxy sizes and types, as well as the overall shapes and correlations between observed features in the baryonic distribution and small kinematic irregularities e.g. Sanders & McGaugh (2002), Famaey & McGaugh (2012), Rodrigues (2014). However, such successful tests are restricted to the range of mass scales covered by spiral galaxies; flat rotation curve velocities roughly within the range of 10 to 300 km/s.

To test to validity (or lack thereof) of MONDian gravity schemes, it is desirable to extend the range of astrophysical

scales over which said ideas can be probed. To do this, we give the expected kinematic profiles for pressure supported systems, astrophysical objects spanning from the $10^4 M_\odot$ of globular clusters, to the $10^{16} M_\odot$ baryonic masses of galaxy clusters.

By the term MONDian gravity we shall refer to any extended gravity theory where at $a > a_0$ scales Newtonian gravity is recovered, while the $a < a_0$ regime reproduces MOND dynamics, at the $v \ll c$ limit, where a_0 is Milgrom’s acceleration of $1.2 \times 10^{-10} m/s^2$ e.g. Bekenstein (2004), Capozziello & De Laurentis (2011), Mendoza et al. (2013). Generically for such theories, beyond a radius given by $R_M = (GM/a_0)^{1/2}$ centrifugal equilibrium velocities will become flat at a level of $V = (GMa_0)^{1/4}$. Similarly, for pressure supported systems, beyond around R_M velocity dispersion profiles will stop falling along Newtonian expectations and flatten out at a level of $\sigma_\infty = V/3^{1/2}$, with M the total baryonic mass of a rapidly converging astrophysical system e.g. Milgrom (1984), Hernandez & Jimenez (2012).

Unfortunately, total baryonic mass determinations for astrophysical systems are fraught with uncertainties and systematics which vary for differing classes of astrophysical systems. Hard to determine gas fractions, dust fractions, star formation histories, the presence of multiple and complex stellar populations and unknown stellar mass functions imply mass to light ratios and their radial variations are subject to large empirical errors. However, the expected scalings of both R_M and σ_∞ with M imply the mass can be eliminated to obtain $R_M \propto \sigma_\infty^2$, a relation between the parameters of the directly observable velocity dispersion profiles which can now be directly tested.

By analysing velocity dispersion profiles from Galactic globular clusters recently observed by Scarpa et al. (2007)a,b, Scarpa & Falomo (2010) and Scarpa et al. (2011), henceforth the Scarpa et al. group, and Lane et al. (2009), Lane et al. (2010)a,b and Lane et al. (2011), henceforth the Lane et al. group, elliptical galaxies having high quality 2D kinematics from the ATLAS project, Capellari et al. (2011), Emsellem et al. (2004) and Emsellem et al. (2011), and local galaxy clusters from the SDSS, York et al. (2000), we show that a universal projected velocity dispersion profile $\sigma(R) = \sigma_0 e^{-(R/R_\sigma)^2} + \sigma_\infty$ adequately serves to model the three distinct classes of astrophysical systems. Further, a scaling of $R_M \propto \sigma_\infty^n$ ensues, with $n = 2.12 \pm 0.11$, compatible with the generic expectations of MONDian gravity models of $n = 2$.

In section (2) we present the development of simple first order predictions for the large scale velocity dispersion expected under MONDian gravity, and the corresponding scalings between the parameters describing such velocity dispersion profiles for pressure supported systems. Section (3) includes a description of the data used for sets of velocity dispersion profiles for globular clusters, elliptical galaxies and galaxy clusters, together with the fitting procedure and parameters obtained for the universal velocity dispersion profile proposed. In section (4) we show how the three sets of systems treated, spanning close to 12 orders of magnitude in mass, all neatly follow the proposed universal velocity dispersion profile, and show also how the flattening radii follow an overall scaling consistent with being proportional to the square of the asymptotic velocity dispersion, as predicted generically under MONDian gravity. Section (5) summarises our conclusions.

2 MONDIAN THEORETICAL EXPECTATIONS

Thinking of modified gravity in terms of a Newtonian force law implies a change of regime from the Newtonian expression of $F_N = GM/r^2$ to $F_M = (GMa_0)^{1/2}/r$, occurring at scales of $R_M = (GM/a_0)^{1/2}$, if one wants to model observed galactic dynamics in the absence of any dark matter, e.g. Milgrom (1983). The details of said transition are not clear, beyond the requirements from consistency with solar system dynamics e.g. Mendoza et al. (2011), Milky Way rotation curve comparisons e.g. Famaey & Binney (2005) and Galactic globular cluster modelling e.g. Hernandez et al. (2012), for the transition to be fairly abrupt. Under such schemes, centrifugal equilibrium velocities will tend to the Tully-Fisher value of:

$$V = (GMa_0)^{1/4}, \quad (1)$$

for test particles orbiting a total baryonic mass M . Under the MONDian regime, the relation between centrifugal equilibrium velocities and isotropic velocity dispersion will be only slightly modified with respect to the Newtonian case, to yield:

$$\sigma_\infty = V/\sqrt{3}, \quad (2)$$

e.g. Milgrom (1984), Hernandez & Jimenez (2012). Thus, we can write the isotropic Maxwellian velocity dispersion of a pressure supported system in the MONDian regime as:

$$\sigma_\infty^2 = \frac{1}{3} (GMa_0)^{1/2}. \quad (3)$$

In order to extend the range over which MONDian dynamics can be tested from the scales covered by spiral galaxies, to the much larger ones over which pressure supported systems appear, would require observations of σ_∞ and independent inferences of the total baryonic mass of various systems, to directly test the validity of equation (3) above. Any such undertaking will be hindered by the large theoretical uncertainties in total (and radially changing) mass to light ratios, uncertain gas fractions, and details of the relevant IMFs and star formation histories, which to make matters worse, vary significantly from the ‘‘simple’’ cases of globular clusters, to elliptical galaxies and on to galaxy clusters. One can circumvent such uncertainties and obtain a simpler empirical test by eliminating M from the above equation in favour of R_M to yield:

$$R_M = \frac{3\sigma_\infty^2}{a_0}, \quad (4)$$

which in astrophysical units reads:

$$\left(\frac{R_M}{pc}\right) = 0.81 \left(\frac{\sigma_\infty}{km/s}\right)^2. \quad (5)$$

The above expression now relates only features of the kinematic velocity dispersion profile of an astronomical system, as σ_∞ will be the large scale asymptotic projected velocity dispersion profile, and R_M will be the radial scale at which the velocity dispersion profile becomes flat. The above will only make any sense if observed velocity dispersion profiles do indeed show such morphology, for a ‘‘Keplerian’’ decline in an inner Newtonian region, and a transition to a flat velocity dispersion regime on crossing the R_M threshold. We are inspired to attempt such a comparison across the vast range of scales covered by pressure supported systems by recent results coming from the observed velocity dispersion profiles of Galactic globular clusters, e.g. Scarpa et al. (2010), Scarpa & Falomo (2011) showing precisely such a morphology, and recently shown to comply with Tully-Fisher MONDian expectations, Hernandez et al. (2013a). Indeed, the recent studies by Tortora et al. (2014) and Chae & Gong (2015) shows the inner kinematics of round elliptical galaxies also from the ATLAS catalogue to be compatible with predictions from MONDian dynamics.

In the following section we show a number of velocity dispersion profiles having precisely the morphology described above, for Galactic globular clusters, elliptical galaxies and galaxy clusters, which we will compare to the expectations of equation (5) in section (4).

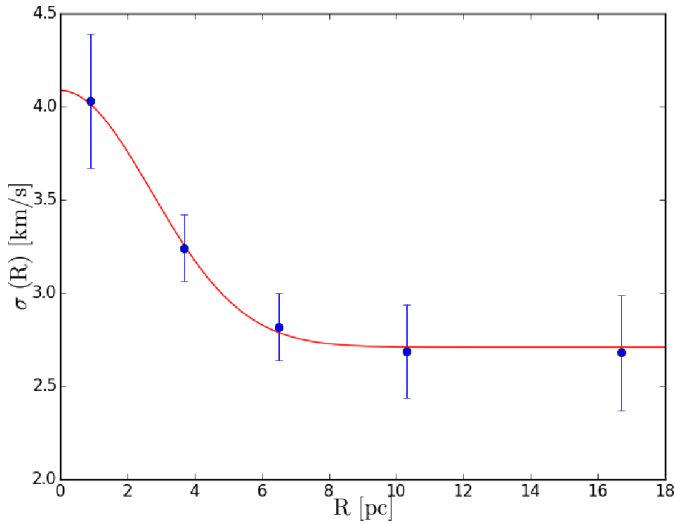


Figure 1. The data show projected velocity dispersion observations with confidence intervals for globular cluster NGC 6171 as a function of radial distance in the system in pc. The solid curve gives the best fit to the universal profile proposed. The adequacy of the fit is evident, in spite of the small number of velocity dispersion measurements available

Notice also that the combination of parameters $R_M \times \sigma_\infty^2 = GM$ is highly reminiscent of the corresponding Newtonian expression, changing R_M for the half mass radius, and σ_∞ for the central velocity dispersion of a purely Newtonian system.

In the above we have assumed that the total baryonic mass has essentially converged, and the dynamical tracers from which σ_∞ is calculated behave as test particles. Although this will never be strictly true, it will hold to a good approximation, given the very centrally concentrated mass profiles of e.g. Galactic globular clusters, the inferred density profiles of close to de Vaucouleurs surface brightness elliptical galaxies, or large scale galaxy populations in galaxy clusters with baryonic distributions often dominated by centrally concentrated x-ray gas. Indeed, pressure supported systems have been accurately modelled recently in the MONDian regime reproducing simultaneously the observed surface brightness profiles and the measured velocity dispersion ones, e.g. Galactic globular clusters by Gentile et al. (2010), the giant elliptical galaxy NGC4649 in Jimenez et al. (2013) and tenuous galactic stellar halos in Hernandez et al. (2013b), all in absence of any otherwise dominant dark matter component.

We end this section with a first order comparison between the relaxation timescales of systems in the Newtonian and the MONDian regimes. For the Newtonian case, relaxation timescales can be estimated from the classical free fall timescale e.g. Binney & Tremaine (1987),

$$\tau_N = (G\rho)^{-1/2}. \quad (6)$$

Similarly, for the MONDian case we can estimate relaxation timescales from the free fall timescale, given this time by the radial scale of the system and the typical equilibrium velocity dispersion, to first order,

$$\tau_M = \frac{R}{(GMa_0)^{1/4}}. \quad (7)$$

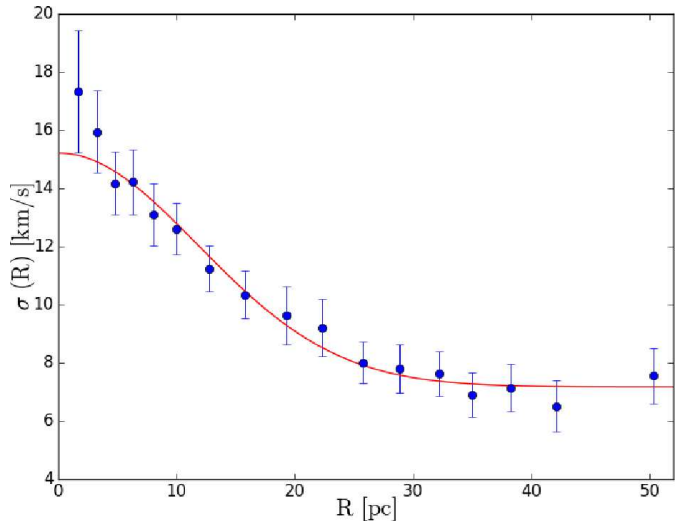


Figure 2. The data show projected velocity dispersion observations with confidence intervals for globular cluster NGC 5139 as a function of radial distance in the system in pc. The solid curve gives the best fit to the universal profile proposed. The high spatial resolution data reveal no significant deviations from the fit.

Writing ρ as M/R^3 in the expression for τ_N , we can obtain the quotient of both timescales as:

$$\frac{\tau_M}{\tau_N} = R^{1/2} \left(\frac{a_0}{GM} \right)^{1/4}, \quad (8)$$

which we can simplify using $R_M = (GM/a_0)^{1/2}$ to obtain:

$$\frac{\tau_M}{\tau_N} = \left(\frac{R_M}{R} \right)^{1/2} \quad (9)$$

Thus, we see that for a system where $R > R_M$, and hence one in the MONDian regime, $\tau_M < \tau_N$, and hence relaxation timescales will be expected to be shorter than in the Newtonian case. This is important for galaxy clusters, typically considered to be marginally relaxed under Newtonian expectations, having $R > R_M$ by a factor of a few (see the following section), would lead us to expect them to be more fully virialized systems under MONDian physics, a natural consequence of the slower fall off in the gravitational force with distance, and consistent with the lack of any multiple components in the galaxy clusters we include in our sample.

3 EMPIRICAL VELOCITY DISPERSION PROFILES

We begin with data for projected velocity dispersion profiles for Galactic globular clusters which have recently become available. In data from the Scarpa et al. group and the Lane et al. group, not only the central values, but the radial projected velocity dispersion profiles for several systems have been published, extending out to several half-light radii. The above authors have shown a flattening of the velocity dispersion profiles for Galactic globular clusters on crossing the a_0 acceleration threshold, in accordance with MONDian gravity expectations. In Hernandez & Jimenez (2012) some of us recently modelled the above globular cluster data to construct self-gravitating models for the systems studied, where both the projected surface brightness profiles

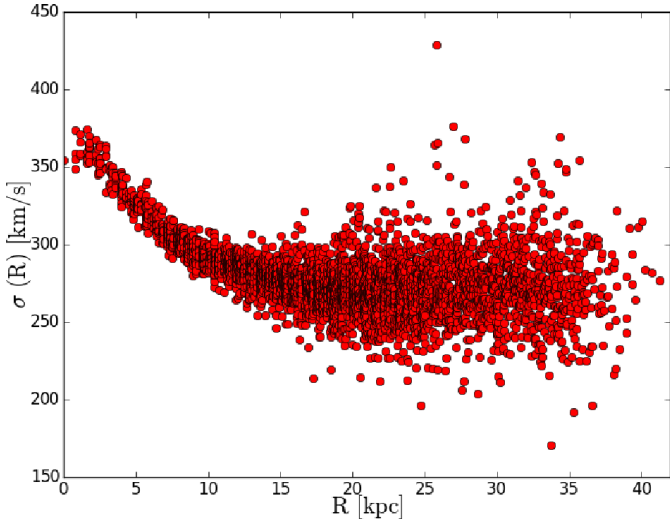


Figure 3. The data show projected 2D velocity dispersion observations for the elliptical galaxy NGC 4486 as a function of radial distance in the system in kpc. Individual confidence intervals are smaller than the plotted points.

and the observed velocity dispersion profiles have been accurately reproduced, using a modified gravity force law of the type described in section (2). Further, in Hernandez et al. (2013a) we showed that the asymptotic velocity dispersion values for the clusters treated actually match the expected scaling of $\sigma_\infty \approx (GMa_0)^{1/4}$ of MONDian gravity, through comparing with stellar synthesis models tuned to the ages and metallicities of each of the individual globular clusters studied. In the above works we also showed that an empirical projected velocity dispersion profile of:

$$\sigma(R) = \sigma_0 e^{-(R/R_\sigma)^2} + \sigma_\infty \quad (10)$$

serves to accurately model the reported velocity dispersion profiles of Galactic globular clusters. In the above profile σ_∞ is the asymptotic value for the systems velocity dispersion, the central value for this quantity is given by $\sigma(0) = \sigma_0 + \sigma_\infty$, and R_σ gives a transition radius beyond which the asymptote is rapidly approached.

Here we include again the fits to the data of the Scarpa et al. and Lane et al. groups to equation (10). We use a non-linear least squares Levenberg-Marquardt algorithm to estimate the parameters, and obtain self-consistent 1σ confidence intervals, which are reported in table (1). We have trimmed the total sample used in Hernandez et al. (2013a) to the 12 globular clusters where the relative errors in the fitted parameters are smallest. This excludes 4 globular clusters with poorly determined velocity dispersion profiles, also keeping the globular cluster sample from growing much beyond the numbers of available well measured systems in the other two categories, extremely low rotation elliptical galaxies and galaxy clusters. This last to ensure that the systematics relevant to any particular class of objects do not dominate and bias the overall comparisons we attempt.

A first example is shown in figure (1), which shows the observed velocity dispersion profile for the Galactic globular cluster NGC 6171 from the Scarpa et al. group, points with error bars. Also shown is the best fit to equation (10), clearly an excellent empirical representation of the measured

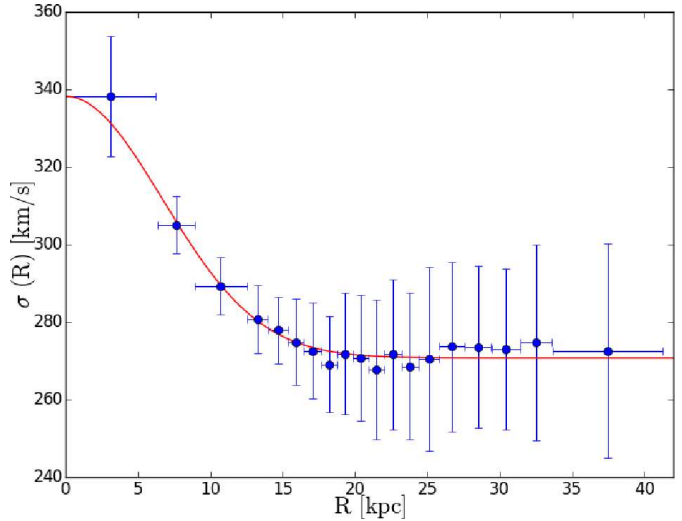


Figure 4. Points with error bars give the radial binning of the data in the previous figure, with vertical error bars showing the 1σ dispersion at each radial bin. The solid curve gives the best fit to the universal profile proposed. The radial scale is in units of kpc. The high resolution allowed by the large data set reveal no significant deviations from the fit.

profile. A clear “Keplerian decline” Newtonian inner region is evident, followed by a transition to a “Tully-Fisher” flat asymptote. Figure (2) gives a second example, for NGC 5139, data also from the Scarpa et al. group. Similarly, the adequacy of the fit is evident for this second, significantly larger system, notice the change in the physical scales of this first two figures.

Next, a sample of low rotation elliptical galaxies was obtained from Capellari et al. (2011) and Emsellem et al. (2004), which form part of the ATLAS 3D survey, in which they have studied the stellar kinematics of 260 early-type galaxies. To ensure that the selected sub-sample was composed of systems with little or no other dynamical support besides velocity dispersion, an analysis from the same survey was used in order to determine a further selection criterion, i.e. the ratio of rotation velocity to velocity dispersion (Emsellem et al. 2011). From here, extremely slow rotators were selected with $V/\sigma < 0.09$ to guarantee a similar dynamical behaviour as the other two classes.

We use the public data from the ATLAS 3D homepage (<http://www-astro.physics.ox.ac.uk/atlas3d/>) and downloaded 2D radial stellar velocity dispersion observations with their respective uncertainties, as well as associated flux for a correct weighted statistical development. From the 2D velocity dispersion observations we extract a projected radial velocity dispersion representation. Due to the large number of pointings in each galaxy, we averaged the projected velocity dispersion observations within 20 radial bins, obtaining an averaged velocity dispersion profile. Each observed point was weighed by luminosity, further reducing uncertainties in our averages. Using again a non-linear least squares Levenberg-Marquardt algorithm, we fit the universal function of eq. (10) to the projected velocity dispersion profiles and obtain the equation parameters as well as their respective confidence intervals. After discarding 4 systems with poorly determined parameters, fractional errors larger than

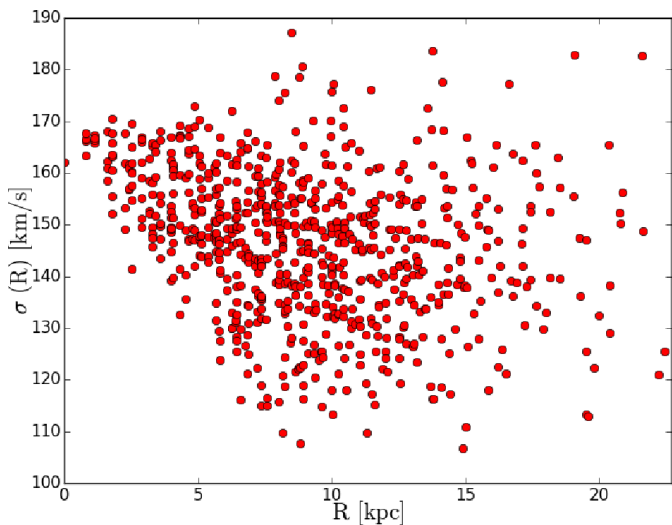


Figure 5. The data show projected 2D velocity dispersion observations for the elliptical galaxy NGC 5831 as a function of radial distance in the system in kpc. Individual confidence intervals are smaller than the plotted points.

50% in the fitted parameters, a final sample of 9 elliptical galaxies results, as reported in table (1).

Two examples of the projected 2D radial velocity dispersion observations are shown in figures 3 and 5, for NGC 4486 and NGC 5831 respectively. The considerable variation in the number of observations, velocity dispersion and radial range is noteworthy. Figures 4 and 6 show the radial binning of the projected 2D radial velocity dispersion of NGC 4486 and NGC 5831 respectively, as well as the best fit to the universal function of equation (10). Note the suitability of the fits in both cases, in the second one, in spite of the large error bars intrinsic to the large dispersion in the data. Galaxies with more rotational support begin to show growing systematic differences to the general shape of equation (10).

For this study, we select a sample of 8 rich Abell Clusters, Abell (1958), that forms part of a larger cluster sample defined by Ibarra-Medel & López-Cruz(2011). These clusters have an Abell Richness Class higher than zero, to ensure having a fair number of galaxies per cluster. Also, we use the redshift range of $0.02 \leq z \leq 0.2$ to sample deep enough inside the cluster luminosity function within the survey magnitude limit. From the 8 Abell Clusters, 3 of them are in common with *The Low-Redshift Cluster Optical Survey* Barkhouse et al. (2007), **LOCOS**. This sample was originally intended to measure optical properties of X-Ray luminous clusters selected from the Einstein sample, Jones & Forman (1999). We use the public data from the Sloan Digital Sky Survey Data Release 7, York et al. (2000). For all selected clusters, we include all galaxies within $30'$ of the reported cluster center. From the SDSS query server (<http://cas.sdss.org/dr7/en/>), we download the redshifts, positions, magnitudes and their associated errors for all galaxies.

We use as a first cluster membership criterion a colour criterion, by selecting all galaxies that lie within the red-sequence of the colour-magnitude diagram e.g. Bower et al. (1992), López-Cruz (1997), López-Cruz et al. (2004). A sec-

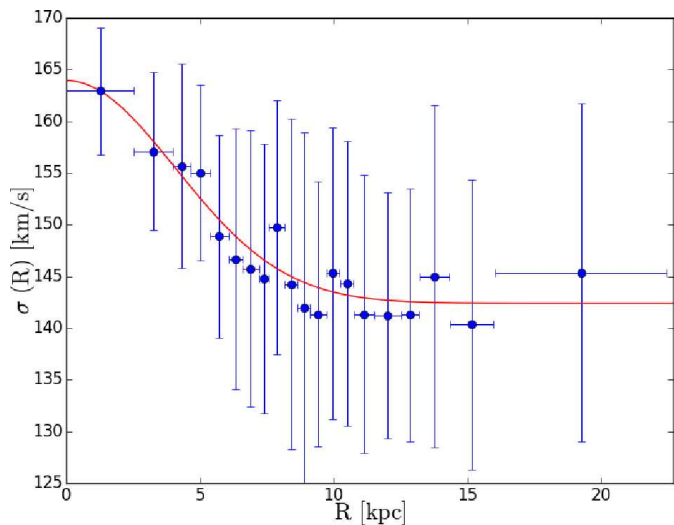


Figure 6. Points with error bars give the radial binning of the data in the previous figure, with vertical error bars showing the 1σ dispersion at each radial bin. The solid curve gives the best fit to the universal profile proposed. The radial scale is in units of kpc. The adequacy of the fit is evident, in spite of the large error bars inherent to this more sparsely sampled system.

ond membership criterion included is based on the Yahil & Vidal (1977) iterative process (the 3σ -clipping method). For each iteration, this procedure selects a new galaxy sub-sample. This process finishes when the velocity limits are the same as the immediate predecessor sub-sample. As the iterative process continues, the contribution of galaxy interlopers rapidly diminishes. At the end of this procedure, the background contribution is zero. In addition, we estimate the cluster centroid of the observed galaxy spatial distribution. In this case, we weighted the galaxy positions by luminosity. Finally, we determine the cluster velocity dispersion within 6 equal concentric rings that cover the first $1.5 Mpc$ of the cluster centre. The selection of the 8 Abell Clusters consists in choosing only those clusters that contain enough galaxies per ring ($N > 10$) to have good statistics. Therefore, this selection criterion ensures a good estimate of the cluster velocity dispersion profiles. The resulting projected velocity dispersion profiles are then fitted to the universal function of equation (10) in exactly the same way as the globular cluster and elliptical galaxy profiles were, to obtain the parameters and confidence intervals reported in table (1).

Two examples are shown in figures (7) and (8), which show the binned projected velocity dispersion profiles for galaxy clusters A 1773 and A 2052, together with the optimal fit to equation (10). Although the error bars are fractionally larger than the ones obtained for the two previous classes of systems, comparison with figures (4), (6), and particularly with figures (1), (2), which have a similar number of radial bins, shows remarkable similarities. If not for the labelling of the scales, this time going up to $1,000 km/s$ and Mpc scales, the observed profiles for the galaxy clusters treated look almost identical to those of Galactic globular clusters and elliptical galaxies. The functional form of equation (10) is clearly an excellent representation of the observed profiles being fitted. These $\sigma(R)$ profiles in the con-

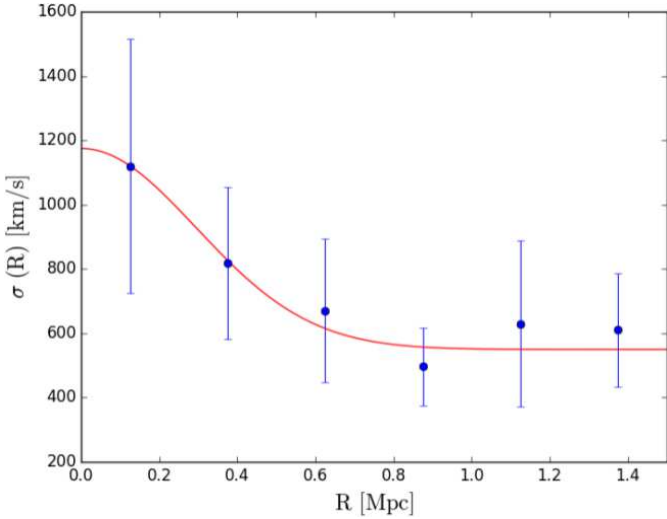


Figure 7. The data show projected velocity dispersion observations for the galaxy cluster A1773 as a function of radial distance in the system in Mpc. The solid curve gives the best fit to the universal profile proposed. The adequacy of the fit is evident, in spite of the vastly larger physical scales over which the system extends, and the large error bars resulting from the much smaller number of galaxies per bin, when compared to the numbers of stars in the cases of globular clusters and elliptical galaxies.

text of galaxy cluster dynamics are of course equivalent to the well known “trumpet” shape in the galaxy density distributions in redshift space e.g. Serra et al (2011).

4 COMPARISONS WITH MONDIAN EXPECTATIONS

We begin this section by noting the vast range of scales over which astronomical pressure supported systems can be fit using the proposed universal projected velocity dispersion profile of eq.(10). Comparing figures (1), (2) with figures (4), (6) and (7), (8), we see that although the physical scale is changing from pc to kpc to Mpc, the observed velocity dispersion profiles are clearly self-similar, appearing as scaled versions of each other.

From eq.(10) we see that the central velocity dispersion values, given by $\sigma(0) = \sigma_0 + \sigma_\infty$, span three orders of magnitude, with the scale radii R_σ covering six orders of magnitude, and the total baryonic masses going from the few $10^4 M_\odot$ scale of the smallest Galactic globular clusters to the almost $10^{16} M_\odot$ of the galaxy clusters containing several hundred galaxies plus x-ray gas included here. If we now scale the projected velocity dispersion profiles of the various systems presented in the previous section, and consider $\sigma(R)/\sigma_\infty$ as a function of R/R_σ for each profile, only one degree of freedom remains, given by the central velocity dispersion, $\sigma(0)/\sigma_\infty$.

Therefore, if we choose distinct systems having fixed $\sigma(0)/\sigma_\infty$ values, they should look identical in a $\sigma(R)/\sigma_\infty$ vs. R/R_σ plot. Figure (9) shows the scaled velocity dispersion profiles of three different systems chosen to have very similar $\sigma(0)/\sigma_\infty$ values. The circles show the Galactic globular cluster NGC 6171, the triangles give data for the elliptical galaxy NGC 5557, while the observed veloc-

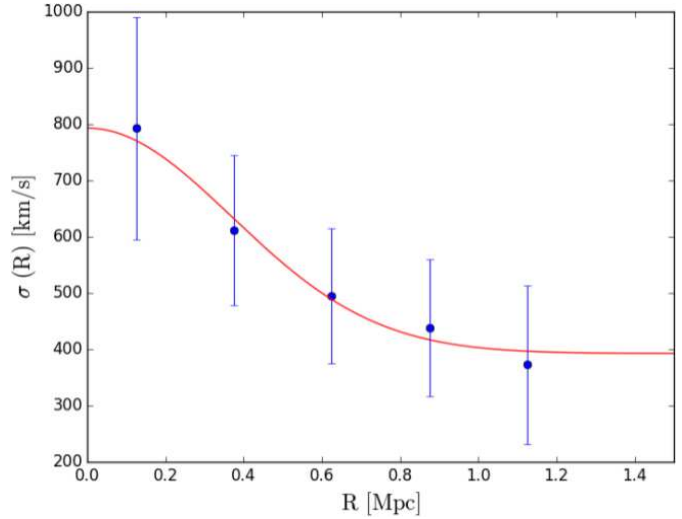


Figure 8. The data show projected velocity dispersion observations for the galaxy cluster A2052 as a function of radial distance in the system in Mpc. The solid curve gives the best fit to the universal profile proposed. The adequacy of the fit is evident, in spite of the vastly larger physical scales over which the system extends, and the large error bars resulting from the much smaller number of galaxies per bin, when compared to the numbers of stars in the cases of globular clusters and elliptical galaxies.

ity dispersion profile for galaxy cluster A 0168 is displayed with squares. The self-similarity of the three quite distinct pressure supported systems is evident, once scaled, all are consistent with each other to within their respective confidence intervals. Actual physical radial scales vary from the $R_\sigma = 3.8pc$ of the globular cluster shown to $R_\sigma = 4.6kpc$ of the elliptical galaxy, to the $R_\sigma = 0.43Mpc$ of the galaxy cluster. The only salient feature is the larger error bars of A 0168, a natural consequence of the much fewer galaxies per radial bin than the millions of stars giving rise to the line widths measured by the ATLAS project for elliptical galaxies, or the large number of stars available in the case of Galactic globular clusters. We see pressure supported systems as showing a simple empirical kinematic profile across many orders of magnitude in scale and distinct classes of systems.

Despite the overlap evident in figure (9), typically we find velocity dispersion profiles for elliptical galaxies to be rather flat, while those of Galactic globular clusters tend to be steeper, with galaxy clusters showing an intermediate morphology, although parameters in the latter case are more poorly constrained. This is illustrated in figure (10), which is analogous to figure (9), but shows more typical examples for the three astrophysical systems analysed, the Galactic globular cluster NGC 7078, the elliptical galaxy NGC4486 and the galaxy cluster A1773. Although the same σ_∞ is evident, the degree of central concentration clearly varies as mentioned above.

We end this section with figure (11), which contains the principal result of our study. The figure shows the R_σ and σ_∞ values for the fits to all of the different pressure supported systems treated, in a logarithmic plane. The systems shown cover a range of $1.8 - 1174km/s$ in central velocity dispersion and $1.8pc - 1Mpc$ in the scale radius R_σ . The

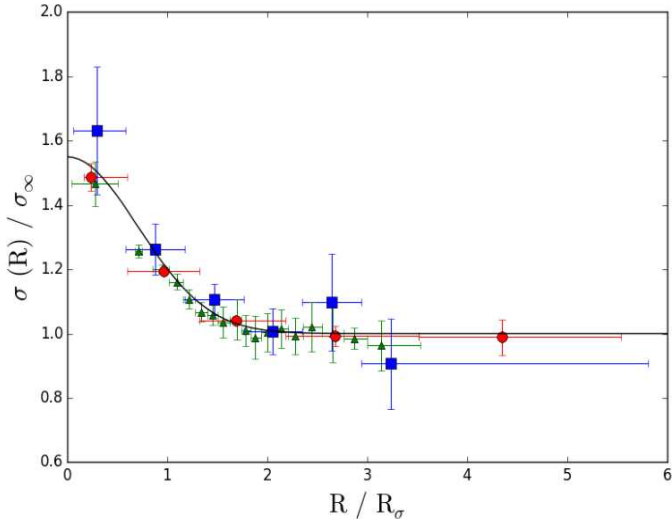


Figure 9. The figure shows observed projected velocity dispersion profiles in units of the corresponding σ_∞ values as a function of radius normalised to the corresponding R_σ values, for three distinct systems. The red circles correspond to measurements for the Galactic globular cluster NGC 6171, with an actual central velocity dispersion of 4.1km/s and $R_\sigma = 3.8\text{pc}$. The green triangles show the elliptical galaxy NGC 5557, with a central velocity dispersion of 282km/s and $R_\sigma = 4.6\text{kpc}$. The blue squares give the profile for the galaxy cluster A 0168, having a central velocity dispersion of 687km/s and $R_\sigma = 0.43\text{Mpc}$. The consistency of the three scaled projected velocity dispersion profiles is evident, despite the vast range of scales covered by the comparison.

three distinct classes of objects are evident, with the small Galactic globular clusters appearing at the low σ_∞ extreme as circles, the galaxy clusters close to the Mpc R_σ extreme with large error bars shown with squares, and triangles at intermediate scales giving results for elliptical galaxies. The solid line is not a fit to the data but gives the $R_M = 3\sigma_\infty/a_0$ prediction of MONDian gravity of equation (4).

In going from volumetric velocity dispersion profiles to the observable projected velocity dispersion profiles, various projection effects intervene, in ways which depend on the details of the degree of central concentration of the volumetric velocity dispersion profile, and the real space density profiles of the tracers being analysed e.g. Hernandez & Jimenez (2012), Jimenez et al. (2013a), Tortora (2014). Such details of the integration implicit in obtaining the line of sight projected profiles we treat necessarily introduce changing systematics across the various classes of systems, from the centrally peaked kinematics of globular clusters to the flatter ones of elliptical galaxies. To the above we must add the systematics inherent to any comparison across such distinct astrophysical systems over such a vast range of distances and observational techniques as what we are attempting here. We thus find it encouraging of the physical interpretation presented that the overall trend evident in figure (11) can be clearly well represented by the predictions of equation (4), under the natural identification of $R_\sigma = R_M$, the transition to the flat velocity dispersion regime being given by the length scale of MONDian gravity. Notice that the trend is much less evident within any particular class of objects, only when combining observations across the many orders

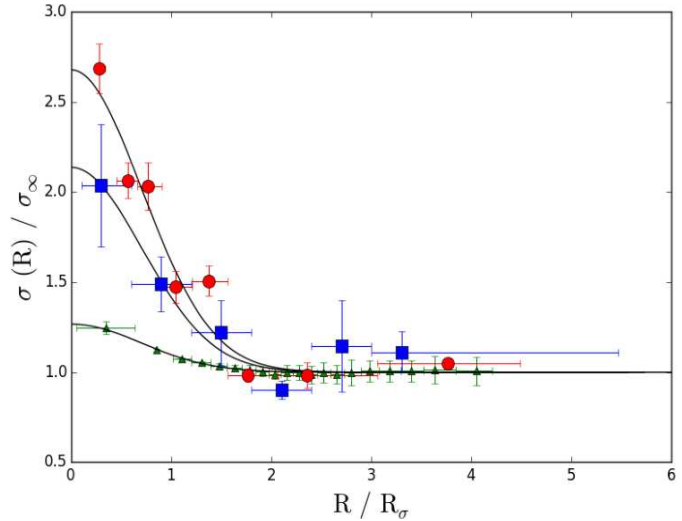


Figure 10. The figure shows observed projected velocity dispersion profiles in units of the corresponding σ_∞ values as a function of radius normalised to the corresponding R_σ values, for three distinct systems. The red circles correspond to measurements for the Galactic globular cluster NGC 7078, with an actual central velocity dispersion of 8.1km/s and $R_\sigma = 8.7\text{pc}$. The green triangles show the elliptical galaxy NGC 4486, with a central velocity dispersion of 344km/s and $R_\sigma = 9\text{kpc}$. The blue squares give the profile for the galaxy cluster A 1773, having a central velocity dispersion of 1174km/s and $R_\sigma = 0.42\text{Mpc}$. The three scaled profiles can be modelled through the same functional form of the proposed universal profile, the figure also shows the tendency for the scaled profiles of elliptical galaxies to be flatter, for globular clusters to be steeper, and for galaxy cluster to be intermediate, for the three classes analysed.

of magnitude covered in figure (11) does the scaling become clear.

We also performed a linear fit to the data in figure (11), but in order to maintain approximately equal weight for all three classes of objects, a fixed average error of 0.2 in the logarithm was used for all data points. Otherwise the galaxy clusters, important systems probing the upper limit of the data range but with more poorly determined parameters, would be entirely ignored by the fit. Such a linear fit to the full data set of figure (11) yields $R_\sigma = (0.57 \pm 0.27)\sigma_\infty^{2.12 \pm 0.11}$, in clear accordance with the predictions of equation (5) for $A = 0.81$ and $n = 2$.

It appears that a unique gravitational physics applies, with a clear transition radius at an R_M scale where the “Keplerian decline” of the inner Newtonian $R < R_M$ region gives way to the “Tully-Fisher” $\sigma(R) \propto (GMa_0)^{1/4}$ of the outer MONDian region, regardless of the fact that we start with self-gravitating systems of stars at pc and kpc scales, to galaxies moving as trace particles in the potential largely determined by hot gas in the largest galaxy clusters analysed.

It is interesting to interpret the slight systematics seen in the figure, for elliptical galaxies to appear slightly above the MONDian prediction, and for galaxy clusters to appear below, in terms of the details of each system. Even though under MONDian physics relaxation timescales will be shorter than in the Newtonian case, see equation (9), still some deficit in σ_∞ at galaxy cluster scales could be the

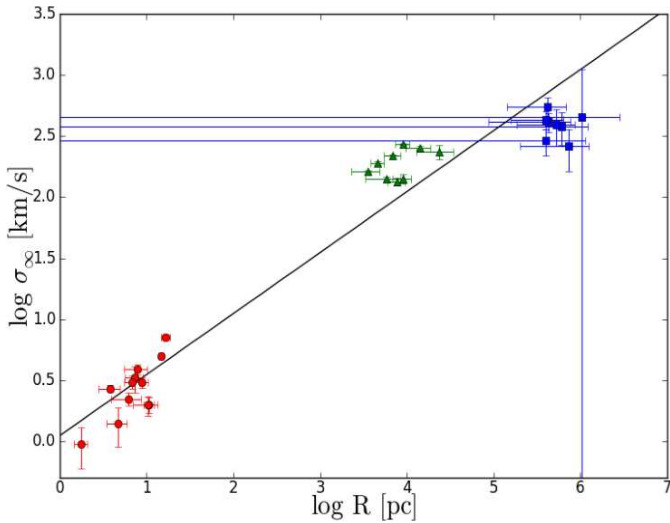


Figure 11. The figure shows σ_∞ and R_σ values for all the systems treated, red circles for Galactic globular clusters, green triangles for extremely low rotation elliptical galaxies and blue squares for galaxy clusters, in a logarithmic (R, σ) plane. The solid line is not a fit to the data, but actually shows the MONDian expectations of equation (4) for the predicted scaling of $R_M = 3\sigma_\infty^2/a_0$, $R_M/pc = 0.81(\sigma_\infty/kms^{-1})^2$. A linear regression fit gives $R_\sigma = (0.57 \pm 0.27)\sigma_\infty^{2.12 \pm 0.11}$, clearly compatible with the theoretical expectation under the identification of $R_\sigma = R_M$.

result of incomplete virialization, although care was taken to include only clusters with no evident multi-component morphology. Similarly, elliptical galaxies could still be affected by the slight rotation present to yield slightly smaller R_σ values. The above suggestion is plausible when we consider the case of Galactic globular clusters, where neither of the two effects mentioned appears, and the systems fall squarely on the predictions of equation (4). Of course, other observational systematics could be at play, which will be not be treated in this first introductory study on the subject, and will be explored in further papers.

Extending the sample to validate our conclusions is evidently a desirable development, which however must be undertaken with care to keep the number of objects at each class considered relatively balanced, to make sure that systematics inherent to any particular class are not biasing conclusions. Also, it is important to restrict the sample to non-rotating systems, elliptical galaxies from the ATLAS sample having v/σ values larger than 0.09 begin to deviate from the proposed profile of equation (10), and systematically more so as v/σ values increase. Similarly, filling the gap present at σ_∞ values of between 10 and 100 km/s would be highly desirable.

5 CONCLUSIONS

A universal projected velocity dispersion profile of $\sigma(R) = \sigma_0 e^{-(R/R_\sigma)^2} + \sigma_\infty$ has been shown to accurately model three distinct classes of astronomical systems; globular clusters, extremely low rotation elliptical galaxies and galaxy clusters.

MONDian gravity generically predicts $R_M = 3\sigma_\infty^2/a_0$, $R_M/pc = 0.81(\sigma_\infty/kms^{-1})^2$. Data across 12 orders of mag-

nitude in mass gives $R_\sigma/pc = A(\sigma_\infty/kms^{-1})^n$, with $A = 0.57 \pm 0.27$ and $n = 2.12 \pm 0.11$.

Thus, in spite of significant observational uncertainties and varying projection effects across apparently very different classes of astronomical systems, the identification of the local physical R_M radius with the empirical projected kinematical R_σ parameter yields results consistent with generic modified gravity expectations, where gravitational anomalies in the $a < a_0$ regime stem from changes in the physics and not a hypothetical dark matter component.

ACKNOWLEDGEMENTS

Xavier Hernandez acknowledges financial assistance from UNAM DGAPA grant IN100814. Reginaldo Durazo acknowledges financial assistance from a CONACyT scholarship.

REFERENCES

- Abell, G.O., 1958, ApJS, 3, 211
 Barkhouse W. A., Yee H. K. C., Lopez-Cruz O., 2007, ApJ, 671, 1471
 Bekenstein J. D., 2004, Phys. Rev. D, 70, 083509
 Binney, J., Tremaine, S., 1987, Galactic Dynamics (Princeton University Press, Princeton, NJ)
 Bower, R. G., Lucey, J.R., & Ellis, R.S. 1992, MNRAS, 254, 601
 Cappellari et al., 2011, MNRAS, 413, 813
 Capozziello S., De Laurentis M., 2011, Phys. Rep. 509, 167
 Chae K.H., & Gong I.T., (2015), MNRAS in press, arXiv:1505.02936
 Emsellem et al., 2004, MNRAS, 352, 721
 Emsellem et al., 2011, MNRAS, 414, 888
 Gentile G., Famaey B., Angus G., Kroupa, P., 2010, A&A, 509, 97
 Hernandez X., Jiménez M. A., 2012, ApJ, 750, 9
 Hernandez X., Jiménez M. A., Allen C., 2013a, MNRAS, 428, 3196
 Hernandez, Jiménez M. A., Allen C., 2013b, ApJ, 770, 83
 Ibarra-Medel, H. J., & López-Cruz, O. 2011, RevMexAACSeries, 40, 64
 Jimenez M. A., Garcia G., Hernandez X., Nasser L., 2013, ApJ, 768, 142
 Jones, C., & Forman, W. 1999, ApJ, 511, 65
 Famaey B., Binney J., 2005, MNRAS, 363, 603
 Famaey B., McGaugh S.S., 2012, LRR, 15, 10
 Lane R. R., Kiss L. L., Lewis G. F., Ibata R. A., Siebert A., Bedding T. R., Szekely P., 2009, MNRAS, 400, 917
 Lane R. R. et al., 2010a, MNRAS, 406, 2732
 Lane R. R., Kiss L. L., Lewis G. F., Ibata R. A., Siebert A., Bedding T. R., Szekely P., 2010b, MNRAS, 401, 2521
 Lane R. R. et al., 2011, A&A, 530, A31
 Lopez-Cruz, O. 1997, Ph.D. Thesis,
 Lopez-Cruz, O. 2001, Revista Mexicana de Astronomia y Astrofisica Conference Series, 11, 183
 López-Cruz, O., Barkhouse, W. A., & Yee, H. K. C. 2004, ApJ, 614, 679
 McGaugh S.S., (2012), AJ, 143,40
 Mendoza S., Hernandez X., Hidalgo J. C., Bernal T., 2011, MNRAS, 411, 226
 Mendoza S., Bernal T., Hernandez X., Hidalgo J. C., Torres L. A., 2013, MNRAS, 433, 1802
 Milgrom M., 1983, ApJ, 270, 365
 Milgrom M., 1984, ApJ, 287, 571

Table 1. Parameters for the pressure supported systems treated.

Type of system	Identification	$\sigma_0(km/s)$	$\sigma_\infty(km/s)$	$R_\sigma(pc)$
Globular Cluster	NGC 0104	4.5 ± 0.4	5.0 ± 0.1	14.8 ± 0.9
Globular Cluster	NGC 1851	4.1 ± 1.7	3.9 ± 0.4	7.9 ± 2.3
Globular Cluster	NGC 1904	2.4 ± 0.6	2.0 ± 0.4	10.3 ± 3.3
Globular Cluster	NGC 2419	4.7 ± 0.8	1.0 ± 0.4	1.8 ± 0.3
Globular Cluster	NGC 5139	8.0 ± 0.7	7.2 ± 0.4	16.7 ± 1.9
Globular Cluster	NGC 6171	1.4 ± 0.4	2.7 ± 0.2	3.8 ± 1.1
Globular Cluster	NGC 6218	3.3 ± 0.9	1.4 ± 0.5	4.7 ± 1.2
Globular Cluster	NGC 6341	3.8 ± 0.7	3.1 ± 0.4	6.9 ± 1.4
Globular Cluster	NGC 6656	3.8 ± 1.3	3.3 ± 0.8	7.4 ± 1.7
Globular Cluster	NGC 6752	3.5 ± 0.8	2.0 ± 0.3	10.7 ± 1.4
Globular Cluster	NGC 7078	5.1 ± 1.0	3.0 ± 0.3	8.7 ± 1.7
Globular Cluster	NGC 7099	1.8 ± 0.5	2.2 ± 0.3	6.2 ± 2.3
Elliptical Galaxy	NGC 3608	37.3 ± 16.8	161.5 ± 3.7	$(3.5 \pm 1.3) \times 10^3$
Elliptical Galaxy	NGC 4374	41.3 ± 9.8	253.9 ± 9.3	$(14.3 \pm 4.5) \times 10^3$
Elliptical Galaxy	NGC 4472	60.3 ± 31.3	236.2 ± 32.8	$(23.4 \pm 10.5) \times 10^3$
Elliptical Galaxy	NGC 4486	73.1 ± 16.8	271.3 ± 5.1	$(9.0 \pm 1.7) \times 10^3$
Elliptical Galaxy	NGC 4552	48.7 ± 9.2	218.7 ± 6.5	$(6.9 \pm 1.5) \times 10^3$
Elliptical Galaxy	NGC 5198	60.7 ± 11.3	141.6 ± 11.6	$(9.1 \pm 2.2) \times 10^3$
Elliptical Galaxy	NGC 5557	90.4 ± 19.7	191.6 ± 6.4	$(4.6 \pm 0.8) \times 10^3$
Elliptical Galaxy	NGC 5831	22.0 ± 7.3	142.0 ± 5.4	$(5.8 \pm 2.6) \times 10^3$
Elliptical Galaxy	NGC 6703	57.1 ± 10.1	133.7 ± 9.6	$(7.7 \pm 1.7) \times 10^3$
Galaxy Cluster	A 0168	271.8 ± 229.4	415.5 ± 74.6	$(0.43 \pm 0.34) \times 10^6$
Galaxy Cluster	A 1213	217.5 ± 153.5	379.8 ± 112.1	$(0.61 \pm 0.62) \times 10^6$
Galaxy Cluster	A 1773	625.2 ± 448.2	549.5 ± 102.2	$(0.42 \pm 0.27) \times 10^6$
Galaxy Cluster	A 1939	138.1 ± 243.3	291.5 ± 71.0	$(0.40 \pm 0.73) \times 10^6$
Galaxy Cluster	A 1983	238.7 ± 117.1	261.2 ± 98.0	$(0.73 \pm 0.53) \times 10^6$
Galaxy Cluster	A 2040	429.5 ± 262.4	433.0 ± 70.3	$(0.40 \pm 0.24) \times 10^6$
Galaxy Cluster	A 2052	400.5 ± 207.2	392.7 ± 130.0	$(0.52 \pm 0.34) \times 10^6$
Galaxy Cluster	A 2151	339.7 ± 621.3	453.2 ± 660.0	$(1.04 \pm 1.79) \times 10^6$

The first two columns give the object class and identifier for the systems studied. The following three entries show the parameters of the fits to the observed projected velocity dispersion profiles and their confidence intervals. Data from the Scarpa et al. group and the Lane et al. group for Galactic globular clusters, the ATLAS collaboration for the elliptical galaxies, and the SDSS for the galaxy clusters.

- Rodrigues D. C., de Oliveira P. L., Fabris J. C., Gentile G., 2014, MNRAS, 445, 3823
 Sanders R. H., McGaugh S. S., 2002, ARA&A, 40, 263
 Scarpa R., Marconi G., Gimuzzi R., Carraro G., 2007a, A&A, 462, L9
 Scarpa R., Marconi G., Gimuzzi R., Carraro G., 2007b, The Messenger, 128, 41
 Scarpa R., & Falomo R., 2010, A&A, 523, 43
 Scarpa R., Marconi G., Carraro G., Falomo R., Villanova S., 2011, A&A, 525, A148
 Serra A. L., Diaferio A., Murante G., Borgani S., 2011, MNRAS, 412, 800
 Swaters R.A., Sanders R.H., McGaugh S S., 2010, ApJ, 718, 380
 Tortora C., Romanowsky A. J., Cardone V. F., Napolitano N. R., Jetzer Ph., 2014, MNRAS, 438, L46
 Yahil, A., & Vidal, N. V. 1977, ApJ, 214, 347
 York, D. G., et al. 2000, AJ, 120, 1579